Open access • Proceedings Article • DOI:10.1109/FUSION.1993.518328

Liquid metal MHD and heat transfer in a tokamak blanket slotted coolant channel

Claude B. Reed, Thanh Q. Hua, D.B. Black, I.R. Kirillov ...+3 more authors

Institutions: Argonne National Laboratory

Published on: 11 Oct 1993 - IEEE/NPSS Symposium on Fusion Engineering

Topics: Heat flux, Heat transfer, Liquid metal and Coolant

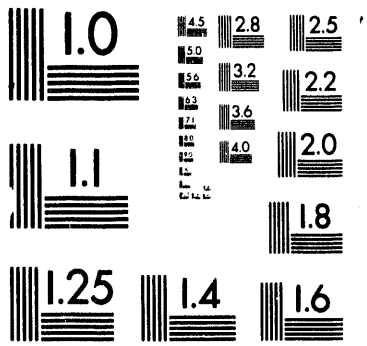
1.0
1.1
1.25
1.4
1.6
1.8
2.0
2.2
2.5
2.8
3.2
3.6
4.0
4.5
5.0
5.6
6.3
7.1
8.0
9.0

1 of 1

ANL/EP/CP--79904
Conf-931018--73

Paper to be presented at the IEEE/NPSS - Fusion 15th Symposium on Fusion Engineering being held in Hyannis, MA, October 12-15, 1993

LIQUID METAL MHD AND HEAT TRANSFER IN A TOKAMAK BLANKET SLOTTED COOLANT CHANNEL[1]

by

Claude B. Reed, Thanh Q. Hua and David B. Black
Fusion Power Program, Engineering Physics Division
Argonne National Laboratory
Chicago,IL 60439, USA

Igor R. Kirillov, Sergei I. Sidorenkov,
Anatoly M. Shapiro and Igor A. Evtushenko
MHD-Machines Laboratory
The D. V. Efremov Scientific Research
Institute of Electrophysical Apparatus
189631 St. Petersburg, Russia

[1]Work supported by the U.S. Department of Energy/Office of Fusion Energy underContract W-31-109-ENG-38.

LIQUID METAL MHD AND HEAT TRANSFER IN A TOKAMAK BLANKET SLOTTED COOLANT CHANNEL[1]

Claude B. Reed, Thanh Q. Hua
and David B. Black
Fusion Power Program
Engineering Physics Division
Argonne National Laboratory
Chicago,IL 60439, USA

Igor R. Kirillov, Sergei I. Sidorenkov,
Anatoly M. Shapiro and Igor A. Evtus' nko
MHD-Machines Laboratory
The D. V. Efremov Scientific Research
Institute of Electrophysical Apparatus
189631 St. Petersburg, Russia

ABSTRACT

A liquid metal MHD (Magnetohydrodynamic)/heat transfer test was conducted at the ALEX (Argonne Liquid Metal Experiment) facility of ANL (Argonne National Laboratory), jointly between ANL and NIIEFA (Efremov Institute). The test section was a rectangular slotted channel geometry (meaning the channel has a high aspect ratio, in this case 10:1, and the long side is parallel to the applied magnetic field). Isothermal and heat transfer data were collected. A heat flux of ~9 W/cm^2 was applied to the top horizontal surface (the long side) of the test section. Hartmann Numbers to 1050 (2 Tesla), interaction parameters to 9×10^3, Peclet numbers of 10-200, based on the half-width of the small dimension (7mm), and velocities of 1-75 cm/sec. were achieved. The working fluid was NaK (sodium potassium eutectic). All four interior walls were bare, 300-series stainless steel, conducting walls.

INTRODUCTION

The slotted channel concept was conceived at NIIEFA (Efremov Institute) as a method for reducing the MHD pressure drop in liquid metal cooled blanket designs [1]. To achieve the full benefits of MHD pressure drop reduction, very high aspect ratio channels have been proposed which require "anchor links" to reduce the effective span of the long side walls and thus lower the bending stresses. Such "anchor links" represent local flow obstructions which may offset the overall performance improvements gained from slotted channel pressure drop reductions. The objectives of this test were to: 1) identify the fusion-relevant conditions under which the thermal-hydraulic performance of a simple slotted channel geometry is well understood and can be modeled; 2) collect thermal-hydraulic performance data from the slotted channel geometry and compare it to both NIIEFA- and ANL (Argonne National Laboratory)-generated pre-test predictions; 3) collect profiles of temperature and velocity, distributions of surface temperature and voltage, and axial pressure gradient data from a portion of the test section which simulates the presence of "anchor links" in a slotted channel; and 4) determine the conditions under which side layer velocity fluctuations are present and assess their beneficial impact on heat transfer enhancement under fusion-relevant conditions.

DESCRIPTION OF TEST SECTION AND TEST CONDITIONS

The test section was designed and fabricated at NIIEFA and tested in ALEX. The geometry of the test section was that of a rectangular slotted channel (meaning the channel had a high aspect ratio, in this case 10:1, and the long side was parallel to the applied magnetic field). The details of the crossection, dimensions, and coordinate system are shown in Fig. 1. The origin for the x-coordinate is the leading edge of the heater block; all lengths are normalized by the duct half-width, 7 mm. The top (heated) wall was 6mm thick; the remaining three walls were made of a thin (1mm) liner which was electrically insulated from its surrounding strongback. All four interior walls were bare, 300-series stainless steel (conducting walls). One of the purposes of the test was to demonstrate that an electrically insulated "sandwich" construction could be used at elevated temperatures to reduce MHD pressure drop. Heat was applied to the top surface to eliminate any buoyancy effects which could arise at the low velocities used here to achieve high interaction parameters [2].

[1]Work supported by the U.S. Department of Energy/Office of Fusion Energy under Contract W-31-109-ENG-38.

The upstream half of the test section (~3m long), was a simple slotted channel with no anchor links, Fig. 1. The downstream half had eight anchor links, Fig. 2. A uniform surface heat flux was provided by tightly clamping a movable aluminum heater block (Fig. 2) to the top surface of the test section. The heater block was powered by four, 3kW each, electric resistance heater rods, embedded into the heater block. An anodized coating on the heater block provided electrical insulation between the test section and the heater block. The heater block was instrumented with twelve TCs (thermocouples) positioned in 0.5 mm dia. by 0.25 mm deep grooves. These TCs provided measurements of the heater block/heated wall interface temperature (z=-1.86). The test section itself was instrumented with fifty-two TCs, as shown in Fig. 3; also embedded in grooves. Except for the TCs in brackets, e.g. [51], the test section TCs measured the NaK/heated wall interface temperature (z=-1.0). Those in brackets measured temperatures in the Z = -1.86 plane.

A traversing ThermalLEVI (Thermal Liquid-Metal Electromagnetic Velocity Instrument) probe was used here for the first time. The design of an ordinary LEVI probe, described in [3], was modified by making the "prongs" from sheathed TCs to produce a ThermalLEVI; a device which can measure both LMMHD velocity and temperature profiles, simultaneously.

Twenty electrodes, Fig. 3, were attached to the bottom (thin) wall of the test section in the vicinity of three of the anchor links. The electrodes were electrically insulated from the surrounding strongback.

Four pressure taps were installed on the bottom wall of the test section; two upstream to measure axial pressure drop without anchor links, and two downstream in the anchor link region. The pressure taps in the anchor link region spanned six anchor links. Table 1 gives a summary of test parameters and Table 2 is the test matrix used. Test matrix conditions will be referred to as they appear in Table 2, e.g. M3P5 is Hartmann number M = ~800. to 1000. and Peclet number Pe= ~200. (The Hartmann number M = BL $(\sigma/\rho\upsilon)^{1/2}$; where σ is the fluid electrical conductivity, ρ is the fluid density, and υ is the fluid kinematic viscosity; the Peclet number Pe = Pr*Re, where Pr is the fluid Prandlt number and Re is the familiar fluid-dynamical Reynolds number based on L.) Temperature rises are taken with respect to the bulk temperature of the upstream fluid coming into the heated region, and normalized by $q''L/k_f$, where k_f is the fluid thermal conductivity.

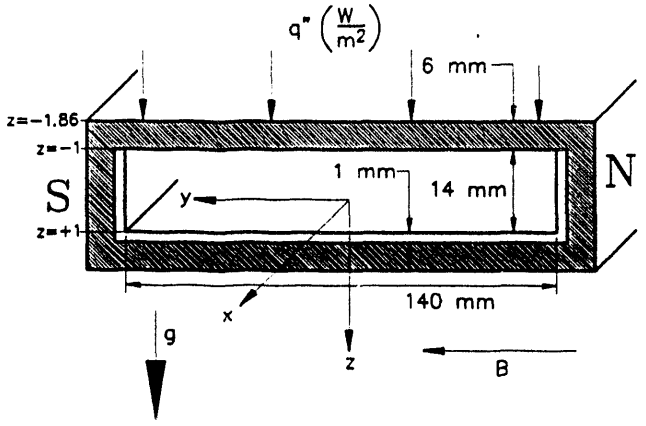

Fig. 1 Slotted Channel geometry.

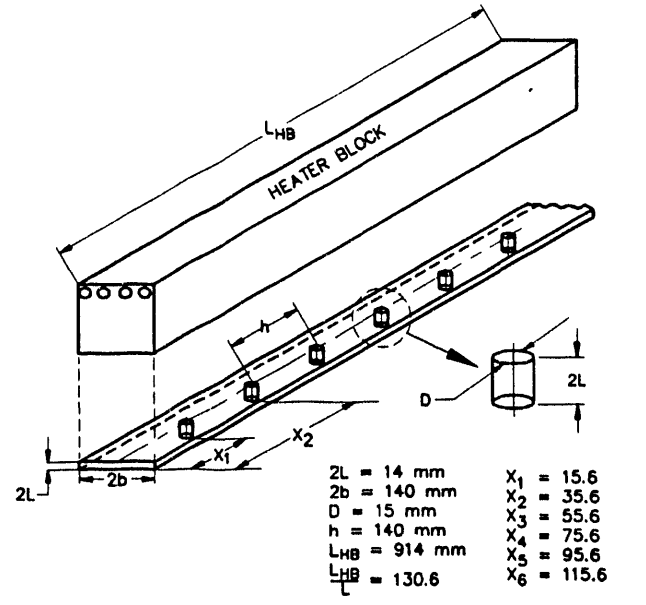

Fig. 2 Anchor link and heater block geometry.

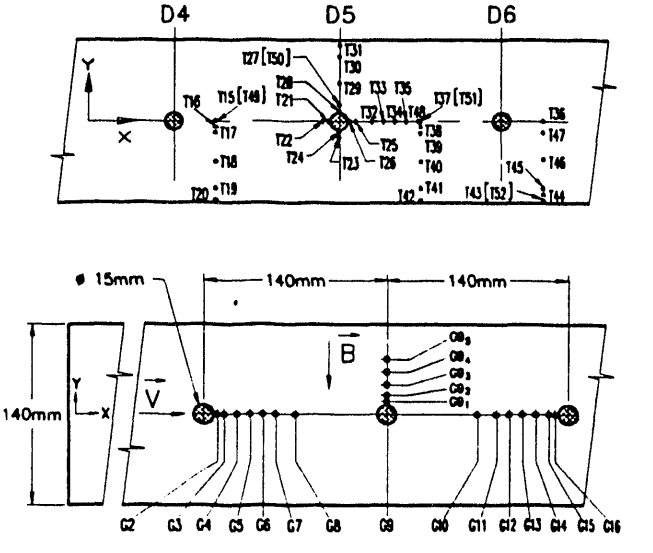

Fig. 3 Electrode and thermocouple geometry with respect to anchor links.

Table 1. Parameter Range for Joint US/Russian MHD-HT Experiment

"Radial" Dimension	14 mm
"Toroidal" Dimension	140 mm
Heated Length	0.914 m
Interaction Parameter	30-10^4 (NaK, L=7 mm)
Hartmann Number	400-1050
Peclet Number	12-200
Average Coolant Velocity	0.05-0.7 m/s
Surface Heat Flux	0.85-0.95x10^5 W/m^2
Heater's Wall Temperature	100-250°C
Temperature Drop Across Heated Wall	< 30°C
Bulk Temperature Rise	< 60°C

Pretest theoretical predictions were prepared by both NIIEFA and ANL. The two analytical approaches are somewhat different but yield essentially the same results at high M and N (interaction parameter $N = \sigma B^2 L/\rho U$). Both sets of predictions were developed for this specific test section geometry, but neither treats the presence of anchor links. Thus all theoretical curves used here are for the case of no anchor links, even though the data may have been acquired in the presence of anchor links.

Table 2. Nominal Test Matrix for Slotted Channel

M / Pe	M3 B=2T M=800	M2 1.0 M=400	M0 M=0
Pe_1=12.4 GPM=1.44 U=4.6 cm/s	N=2000		
Pe_2=25 GPM=2.9 U=9.2 cm/s	N=1000		
Pe_3=50 GPM=5.8 U=18.4 cm/s	N=500		
Pe_4=100 GPM=11.5 U=36.8 cm/s	N=250		
Pe_5=200 GPM=23.1 U=73.6 cm/s	N=125	N=7.8	N=0

ISOTHERMAL RESULTS

LEVI velocity profiles were collected for M3P3, M3P4, and M3P5. Fig. 4 shows a profile for M3P5, which is representative of all three conditions. The small size of the test section in the z-direction, 14 mm, restricted the range in the z-direction over which the ThermalLEVI probe could be traversed, thereby limiting the data collection region to $-0.86 < z < 0.0$. Fig. 4 also shows theoretical velocity profile predictions from NIIEFA. Profiles are shown for three y values; y = 0.0, y = 5.1, and y = 8.3. The agreement is good everywhere except inside the wall jet layer. It is possible that the size of the probe is so large that locally the side layer flow is disturbed by the presence of the probe, and thus a lower velocity is measured. It is also possible that the presence of velocity fluctuations observed in the sidelayer for these three conditions served to increase the average width of the sidelayer and reduce the average velocity therein.

Axial pressure drop data at two Hartmann numbers, M=400. and M=820. with and without anchor links are shown in Fig. 5. The experimental value of the dimensionless pressure gradient ($dP/dx\sigma UB^2$) was divided by the theoretical value obtained from ANL pretest predictions; a value of unity indicates exact agreement. It can be seen that the pressure drop without anchor links is about 10% to 25% higher than predicted at the high Hartmann number, and somewhat higher at M=400. This result suggests that the three thin conducting sidewalls are substantially electrically insulated from their strongback, as intended. The presence of anchor links produces a pressure drop from 50% to 75% higher than the no-anchor-link theory at M=820. Data at higher interaction parameters are needed to determine if the vague trend toward lower pressure drops suggested by Fig. 5 is borne out.

Figs. 6 and 7 present the electrode distributions for the same two Hartmann numbers as above and several interaction parameters as shown. Note in these two figures only, the distances are normalized by b=70 mm, half the long side wall dimension, see Fig. 1. Fig. 6 shows the effect of N on the lateral distribution of voltages in the thin bottom wall at the x=75.6 plane (anchor link D4, see Fig. 3). It can be seen that the distributions become invariant above N=~1000., indicating that flow in this plane has become inertialess. Fig. 7 combines electrode distributions taken downstream of anchor link D3, with those upstream of D5. In Fig. 7, negative values of the abscissa are from electrodes G10-G16 (upstream) and positive abscissa are

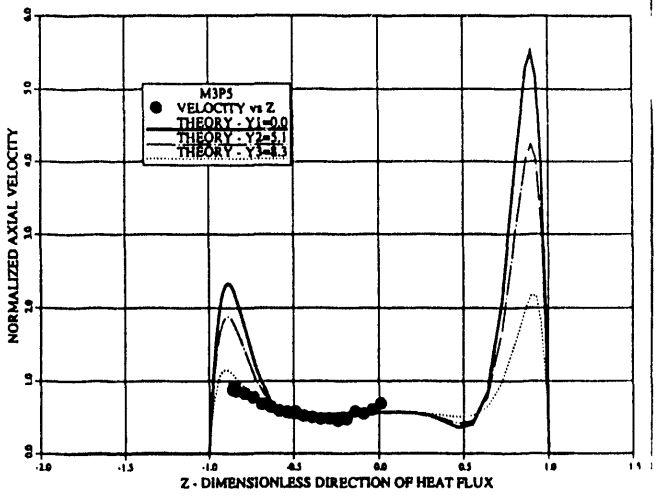

Fig. 4 LEVI velocity profile: comparison of NIIEFA theory: and measurements for M3P5 at x=65.3 without anchor links.

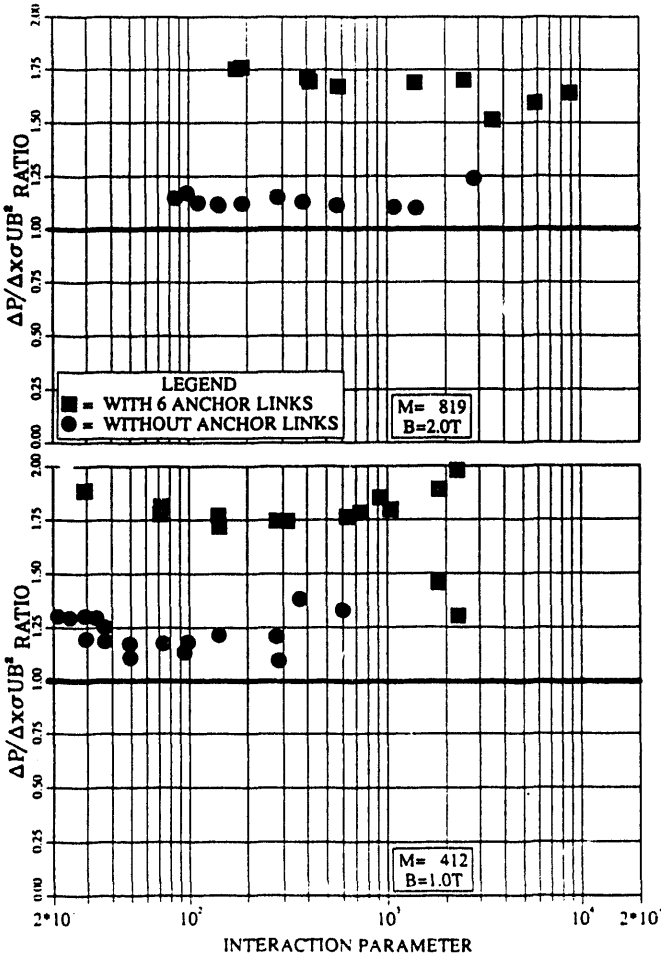

Fig. 5 Comparison of measurements and ANL theory: axial pressure drop data in slotted channel with and without anchor links.

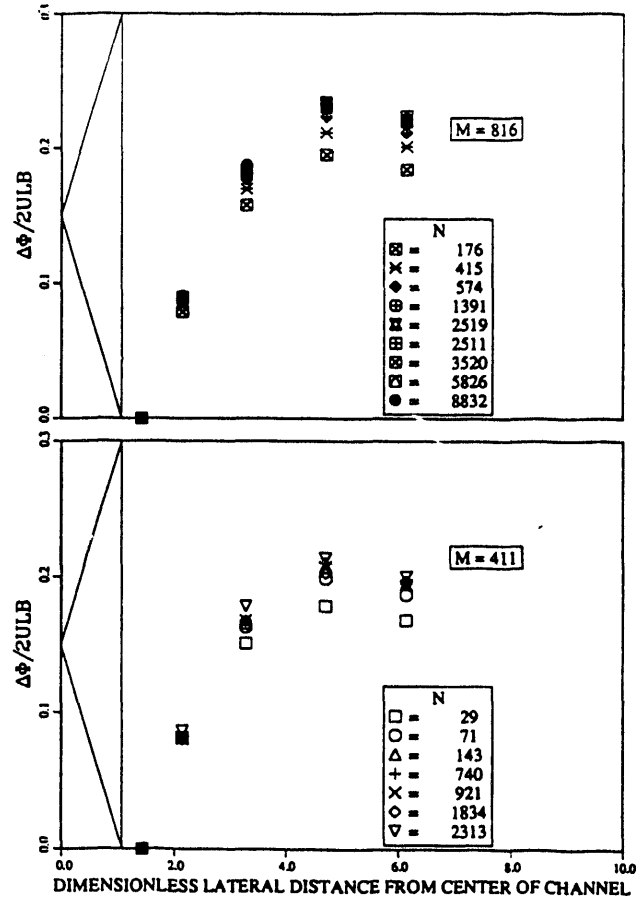

Fig. 6 Lateral distribution of bottom wall electrode voltages in the plane of an anchor link (x=75.6).

from G2-G8 (downstream). The downstream electrode distributions, as in Fig. 6, are invariant above N = ~1000. The upstream distributions may not have become invariant for even the highest values of N achieved here. The effect of Hartmann number on the electrode distributions seems minimal, for the two values of M reported here.

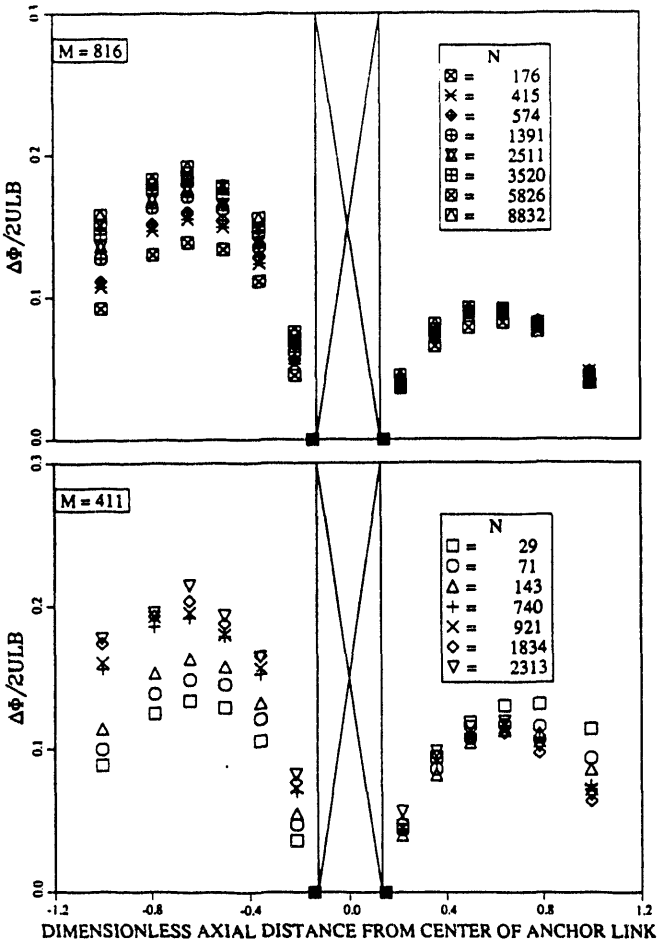

Fig. 7 Axial distribution of bottom wall electrode voltages along test section centerline (z=0) upstream and downstream of an anchor link.

HEAT TRANSFER RESULTS

The ThermalLEVI probe was used to measure temperature profiles in the vertical midplane of the channel (y=0), at the axial location x=65.3; see Figs. 8-10. In Fig. 8, profiles are shown for M0P5, M2P5, and M3P5; these three temperature profiles show the effect of increasing the magnetic field while keeping Pe constant. It can be seen that as the magnetic field increases, the temperature profile becomes more and more flat. This means that the heat transfer is improved by the magnetic field. For this particular geometry, the improvement comes from a combination of high average velocity and large velocity fluctuations (both in the MHD sidelayer).

Also plotted on Fig. 8 is a curve labeled "Perfect Mixing", which was simply calculated from heat balance considerations assuming no heat loss. The temperature profiles were also integrated to estimate the average fluid temperature; this average temperature was compared to the "Perfect Mixing" temperature to give an idea of the importance of heat losses, 3-D effects, and axial conduction effects at the low Pe used in some of the conditions here. Since heat losses were estimated to be of the order of 3 %, any remaining disagreement between the two numbers is probably due to 3-D effects or axial conduction effects. Table 3 gives the ratio of the integrated average temperature divided by the "Perfect Mixing" temperature. It appears that the M2P5 case suffers from some 3-D effects due to the low value of M. The Re corresponding to the P5 condition is only ~6000.; hence the low ratio of temperatures for M0P5 is probably due to non-MHD 3-D effects resulting from non-fully developed turbulent flow. Departures at lower values of Pe are probably due to axial conduction effects.

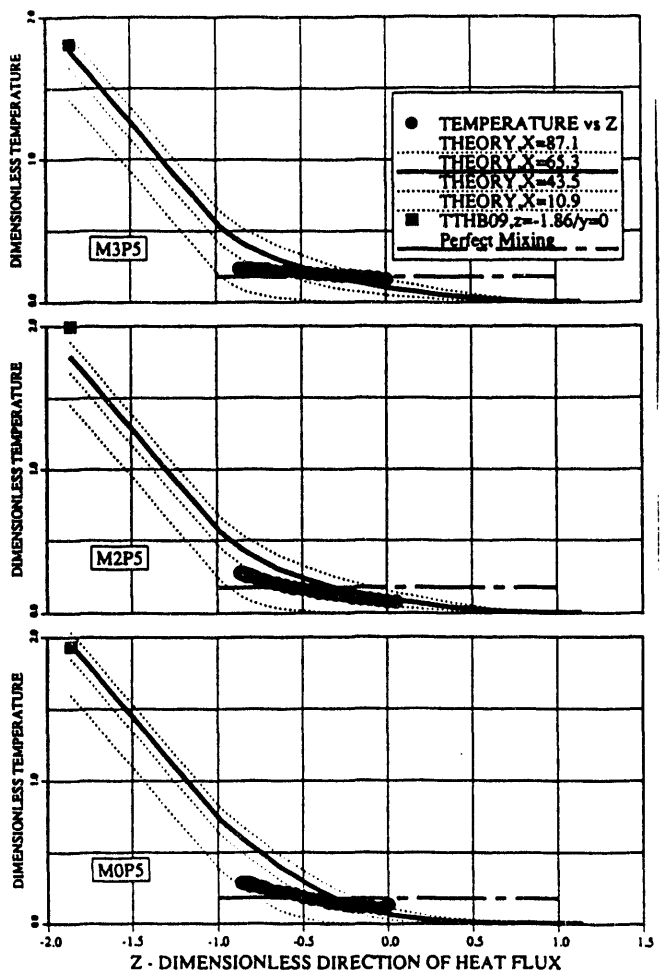

Fig. 8 ThermalLEVI temperature profiles for M0P5, M2P5, and M3P5 for x=65.3.

Table 3. Average Temperature Ratio

M / Pe	800	400	0
12.5	0.86	-	-
25	0.78	-	-
50	0.79	-	-
100	0.90	-	-
200	0.90	0.64	0.71

In Fig. 9 temperature profiles are shown for M3P5, M3P3, and M3P2; these three profiles show the effect of decreasing Pe (increasing N) while keeping the magnetic field constant. Here it can be clearly seen that the data approach the theoretical predictions as N approaches ~1000. From other measurements, not reported here, it was found that fluctuations in the sidelayer were damped as N approached ~1000., hence the good agreement between theory (which assumes no fluctuations) and data at high N.

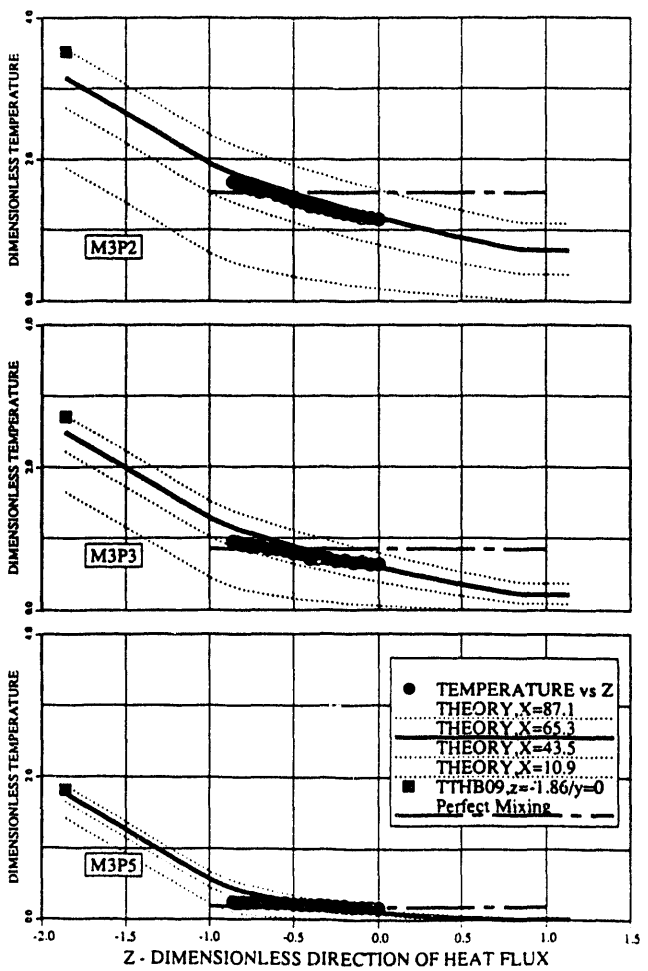

Fig. 9 ThermalLEVI temperature profiles for M3P5, M3P3, and M3P2 for x=65.3.

Following a suggestion by L. Barleon [4], a simple model for slug flow laminar heat transfer was used to fit temperature profiles from the measurements. The temperature distribution, according to this model is as follows:

$$\theta(z,x) = 2q''/\lambda\{(a\cdot x/\pi)^{1/2} \cdot e^{-z^2/4ax} - z/2\ erfc\ z/(2\sqrt{ax})\}$$

$$\theta = T - T_o \text{ and } a = \lambda/(U\rho c_p)$$

$$\theta_1(z = 0\ ,\ x) = 2q''\ (1/\pi U\rho c_p)^{1/2} \cdot x^{1/2}$$

The model was used to "back-calculate" the "effective thermal conductivity" λ which can be associated with a given test matrix condition. Fig. 10 shows the fit of the above equation to the profile for M3P5. Table 3 gives the ratio of λ divided by the ordinary, thermophysical value of the thermal conductivity. The vertical columns are for constant M, and the horizontal rows are for constant Pe. To first order, this table answers the question which has been asked so often for the past few years: "Is MHD heat transfer better or worse than laminar slug flow heat transfer?". The values in Table 4 show that the heat transfer can be up to 5.7 times better than laminar slug flow.

Another, perhaps more impressive, way to look at these results is to normalize the values in Table 4 by the turbulent value, i.e., the effective thermal conductivity determined for M = 0, Pe = 200. Those results are shown in Table 5. Based on this normalization, in very qualitative terms, one could say that MHD heat transfer in a slotted channel is 1.2-1.3 times better than turbulent flow. The relative effects of the side layer and the side layer fluctuations here require much further discussion and interpretation. The entire topic of the existence and importance of the sidelayer fluctuations will be the subject of a future publication. Therefore, when discussing these results, one should remember the complex nature of the flow and the simplicity of the model.

The solid square symbol appearing in Figs. 8-10 (plotted at z = -1.86) represents the heater block/heated wall interface temperature at y = 0 and x = 65.3. This temperature is expected to fall on the tip of the heavy

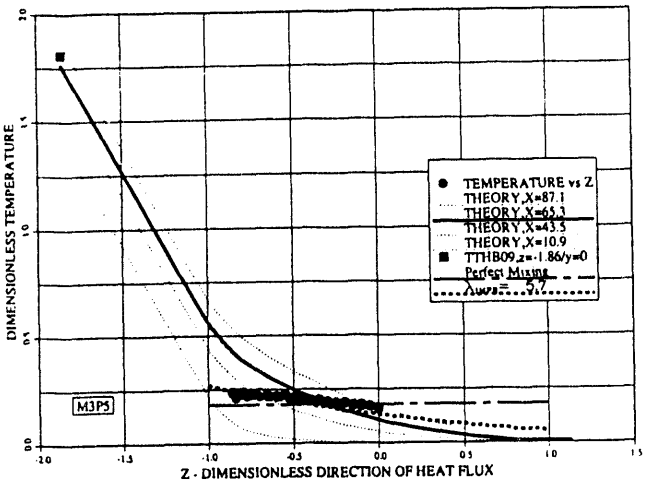

Fig. 10 ThermalLEVI temperature profile: comparison with slug flow model, M3P5.

solid curve labeled "Theory, X = 65.3." In general there is good agreement on this point.

Figs. 11-15 present various metal surface temperature distributions both with and without anchor links. The same three test matrix conditions are used consistently throughout the five figures to show the effects of both M and Pe: M0P5 (bottom), M3P5 (middle), and M3P2 (top); refer to Table 2. Also consistently throughout the five figures (except for Fig. 13), the same symbol (bullet) is used for anchor link data, while an open circle is used for non-anchor link data. NIIEFA theoretical predictions are shown on all figures as appropriately labeled curves.

Table 4. Thermal Conductivity Ratio, laminar slug flow = 1

M / Pe	800	400	0
12.5	0.55	-	-
25	1.10	-	-
50	1.83	-	-
100	3.92	-	-
200	5.7	5.26	4.53

Table 5. Effective thermal conductivity ratio, turbulent flow = 1

M / Pe	800	400	0
12.5	0.12	-	-
25	0.21	-	-
50	0.40	-	-
100	0.87	-	-
200	1.26	1.16	1

Fig. 11 shows axial distributions of centerline (y=0) temperature at the heater block/test section interface (z=-1.86) with and without anchor links for the three test matrix conditions. It can be seen that the temperature with anchor links is consistently higher than without them. At high Pe, the results seem almost identical, the anchor links causing perhaps a 30% penalty in temperature rise; but at low Pe, the effect is more pronounced, costing roughly an additional unit of dimensionless temperature rise everywhere along the length of the heater block.

This picture changes, however when one examines the axial distributions of the corner region (y=8.29) temperature at the heater block/test section interface (z=-1.86) with and without anchor links, Fig. 12. Here it can be seen that except for some perturbation near the inlet region ($x < \sim 30$), the distributions are roughly the same, although some influence due to the anchor links may be evident at the farthest downstream measurement point.

Fig. 13 shows greater detail of the axial distribution of the centerline (y=0) temperature on each side of the heated wall (z=-1.0) & (z=-1.86) in the immediate vicinity of an anchor link. The picture suggested here is roughly consistent with that from Fig. 11, i.e., there is some penalty to be paid at high Pe, but more so (roughly one unit) at the low Pe. In this figure, the bullet symbols represent data taken at the NaK-heated wall interface, the open circles taken at the heater block-heated wall interface.

At axial positions x=80.6 and x=95.6, lateral temperature profiles were measured at the heated wall-NaK interface, with and without anchor links. The results are shown is Figs. 14 and 15. NIIEFA theoretical curves (without anchor links) are plotted for four axial (x) positions to give the reader a perspective

on the temperature variation along the axial direction as well as in the lateral direction. These two figures seem to suggest that at the two high Pe conditions, the presence of anchor links produce uniform but lower temperatures in the lateral regions away from the immediate vicinity of the anchor links. At the low Pe condition, the lateral uniformity in temperature persists, but the magnitudes have increased to become roughly equal to the non-anchor link distributions. These data, then, seem to suggest that the adverse thermal effects of the anchor links are confined to the central plane of the slotted channel, where the anchor links are perturbing the flow; in the remainder of the channel (except perhaps for some three-dimensional inlet flow disturbances), the thermal effects of the anchor links are minimal, or possibly even beneficial.

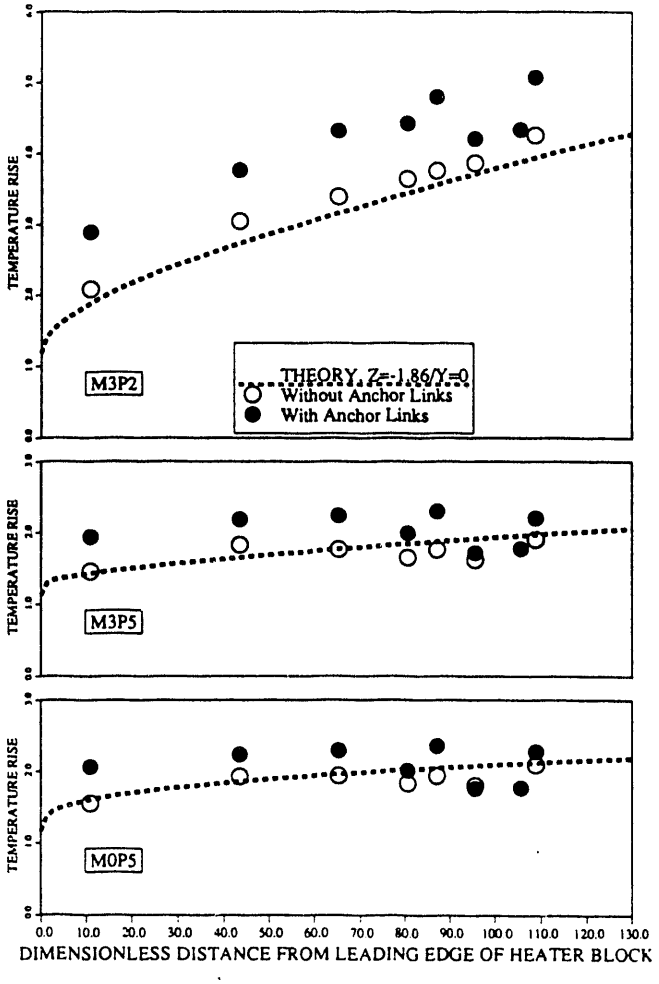

Fig. 11 Comparison of measurements and NIIEFA theory: axial distribution of centerline (y=0) temperatures at heater block/test section interface (z=-1.86).

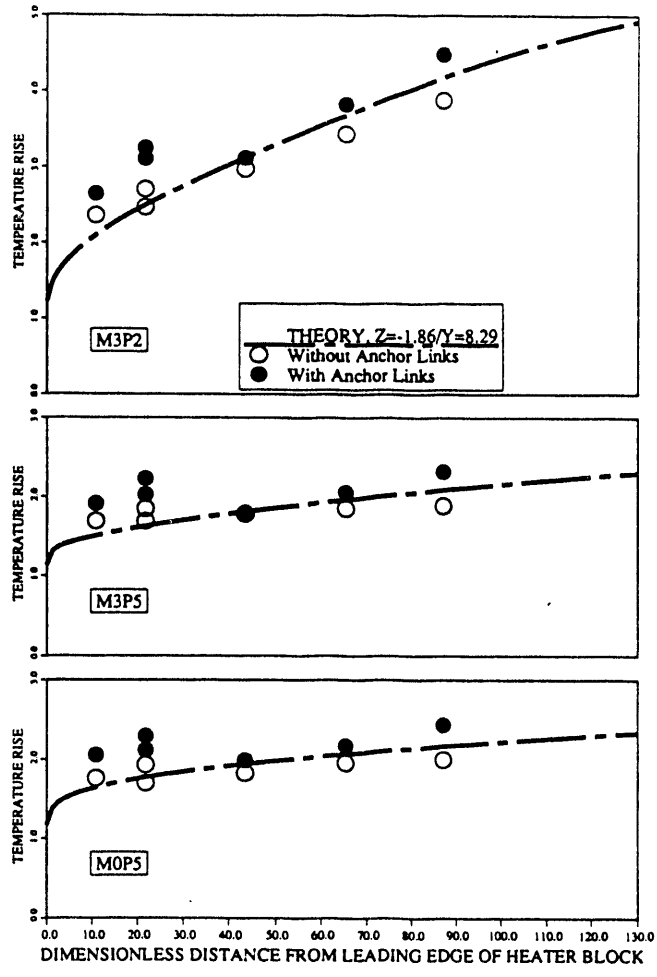

Fig. 12 Comparison of measurements and NIIEFA theory: axial distribution of corner region (y=8.29) temperatures at heater block/test section interface (z=-1.86).

DISCUSSION AND CONCLUSIONS

In the simple slotted channel geometry, under conditions for which the flow was laminar and no side layer velocity fluctuations were present, i.e., M3P2 measurements of temperature and velocity profiles in the flowing NaK agreed well with code predictions from both NIIEFA and ANL; the agreement was similarly good for axial temperature distributions and axial pressure gradients. But in those cases where side layer fluctuations were present, M3P5 for example, the side layer velocity fluctuations had a drastic impact on the temperature profiles in the flowing liquid metal; the effect was to mix the flow to such an extent that the temperature profiles were flatter and heat transfer coefficients were higher than those found even in ordinary turbulent flow.

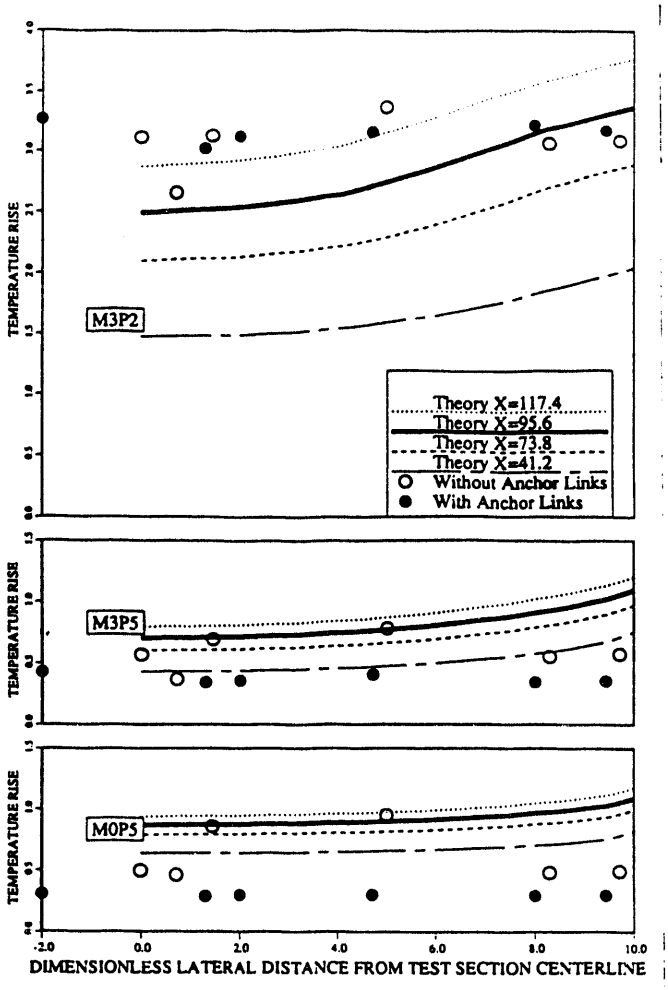

Fig. 15 Comparison of measurements and NIIEFA theory: lateral distribution of temperatures at heated wall–NaK interface (z=−1.0) & (x=95.6).

REFERENCES

[1] I. V. Lavrent'ev, "Liquid metal blanket of fusion tokamak reactor," IV All Union Conference on the Engineering Problems of Fusion Reactors, Leningrad, 1988, pp. 326-327.

[2] S. Kakac and R. Shah, eds., Handbook of Single-Phase Convective Heat Transfer, John Wiley & Sons, 1987, pp. 8.4-8.8 .

[3] C. B. Reed, B. F. Picologlou, P. V. Dauzvardis, and J. L. Bailey, "Techniques for measurement of velocity in liquid-metal MHD flows," Fusion Technology, 10(3), p. 813, 1986.

[4] L. Barleon, private communication, Feb., 1993.

[5] C. B. Reed, B. F. Picologlou, T. Q. Hua, and J. S. Walker, "ALEX results - a comparison of measurements from a round and a rectangular duct with 3-D code predictions," Proceedings of the 12th Symposium on Fusion Engineering, pp. 1267-1270, October, 1987.

DATE
FILMED
2/3/94
END